

Supplementary Material to “Flexible Generalized Low-Rank Regularizer for Tensor RPCA”

Anonymous submission

Abstract

This supplementary material includes a detailed proof of Proposition 1 introduced in the main paper, providing a rigorous mathematical foundation for the theoretical claims. Additionally, it elaborates on the optimization process for the proposed SFGTRPCA model, describing the algorithmic steps. Moreover, it presents additional experimental results that further validate the effectiveness of our proposed models, offering extended analyses and insights into the main paper. Collectively, these materials enhance the confidence of the study’s conclusions and provide a deeper understanding of the methodologies and findings discussed.

Notations and Definitions

First, we introduce the key notations summarized in Table 1 and necessary definitions used in the main text.

Definition 1. (T-SVD) (Kilmer and Martin 2011) For a tensor $\mathcal{X} \in \mathbb{R}^{d_1 \times d_2 \times d_3}$, it can be factorized by t-SVD as

$$\mathcal{X} = \mathcal{U} * \mathcal{S} * \mathcal{V}^T, \quad (1)$$

where $\mathcal{U} \in \mathbb{R}^{d_1 \times d_1 \times d_3}$, $\mathcal{V} \in \mathbb{R}^{d_2 \times d_2 \times d_3}$ are orthogonal tensors, i.e., $\mathcal{U} * \mathcal{U}^T = \mathcal{U}^T * \mathcal{U} = \mathcal{V} * \mathcal{V}^T = \mathcal{V}^T * \mathcal{V} = \mathcal{I}$, and $\mathcal{S} \in \mathbb{R}^{d_1 \times d_2 \times d_3}$ is an f-diagonal tensor, i.e., its frontal slices are the diagonal matrices, and “*” is the t-product.

Definition 2. (Tensor Nuclear Norm, TNN) (Lu et al. 2020) For $\mathcal{X} \in \mathbb{R}^{d_1 \times d_2 \times d_3}$ and $d = \min(d_1, d_2)$, the Tensor Nuclear Norm of \mathcal{X} is defined as

$$\|\mathcal{X}\|_* = \frac{1}{d_3} \sum_{k=1}^{d_3} \sum_{i=1}^d \sigma_i(\bar{\mathcal{X}}^{(k)}), \quad (2)$$

where $\bar{\mathcal{X}}$ is the result by applying FFT on \mathcal{X} along the third dimension, i.e., $\bar{\mathcal{X}} = fft(\mathcal{X}, [], 3)$. $\bar{\mathcal{X}}^{(k)}$ is the k-th slice of $\bar{\mathcal{X}}$, $\sigma_i(\bar{\mathcal{X}}^{(k)})$ is the i-th singular value of $\bar{\mathcal{X}}^{(k)}$, and $d = \min(d_1, d_2)$.

Definition 3. (FGTNN) For a tensor $\mathcal{X} \in \mathbb{R}^{d_1 \times d_2 \times d_3}$, $d = \min(d_1, d_2)$, the Flexible Generalized Tensor Nuclear Norm (FGTNN) is defined as follows

$$\|\mathcal{X}\|_{G,\alpha,*} = \frac{1}{d_3} \sum_{k=1}^{d_3} \sum_{i=1}^d g_\alpha(\sigma_i(\bar{\mathcal{X}}^{(k)})), \quad (3)$$

Notation	Description
$\mathcal{X}, \mathbf{X}, \mathbf{x}, x$	tensor, matrix, vector, scalar
$\mathcal{X} \in \mathbb{R}^{d_1 \times d_2 \times d_3}$	observed 3-order tensor
\mathcal{X}_{ijk} or $\mathcal{X}(i, j, k)$	(i, j, k) -th entry of \mathcal{X}
$\mathcal{X}(i, :, :)$	i-th horizontal slice of \mathcal{X}
$\mathcal{X}(:, j, :)$	j-th lateral slice of \mathcal{X}
$\mathbf{X}^{(k)}$ or $\mathcal{X}(:, :, k)$	k-th frontal slice of \mathcal{X}
FFT	Fast Fourier Transform
$\bar{\mathcal{X}} \in \mathbb{C}^{d_1 \times d_2 \times d_3}$	FFT of \mathcal{X} along the 3-rd dimension
$\bar{\mathcal{X}}^{(k)} \in \mathbb{C}^{d_1 \times d_2}$	k-th frontal slice of $\bar{\mathcal{X}}$
$\ \mathcal{X}\ _*$	Tensor Nuclear Norm (TNN)
$\ \mathcal{X}\ _1$	Tensor ℓ_1 Norm (TLIN)
$\ \mathcal{X}\ _F$	Tensor Frobenius Norm
$\ \mathcal{X}\ _\infty$	Tensor infinity Norm

Table 1: Key notations used in this text.

where $g_\alpha(x)$ is

$$g_\alpha(x) = 2c \cdot \frac{|\alpha - 2|}{\alpha} \left(\left(\frac{|x|/c}{|\alpha - 2|} + 1 \right)^{\alpha/2} - 1 \right), \quad (4)$$

where $\alpha \in \mathbb{R}$ is a continuous parameter that controls the shape of $g_\alpha(x)$ and $c > 0$.

Definition 4. (Weighted Tensor Nuclear Norm, WTNN) (Wang et al. 2023b) For a tensor $\mathcal{X} \in \mathbb{R}^{d_1 \times d_2 \times d_3}$ and a weight matrix $\mathbf{W} \in \mathbb{R}^{d \times d_3}$, $d = \min(d_1, d_2)$, the WTNN of \mathcal{X} is defined as

$$\|\mathcal{X}\|_{\mathbf{W},*} = \frac{1}{d_3} \sum_{j=1}^{d_3} \sum_{i=1}^d W_{ji} \sigma_i(\bar{\mathcal{X}}^{(j)}). \quad (5)$$

Definition 5. (Weighted Tensor ℓ_1 Norm, WTLIN) (Wang et al. 2023b) For a tensor $\mathcal{X} \in \mathbb{R}^{d_1 \times d_2 \times d_3}$ and a weight tensor $\mathcal{W} \in \mathbb{R}^{d_1 \times d_2 \times d_3}$, the WTLIN of \mathcal{X} is defined as

$$\|\mathcal{X}\|_{\mathcal{W},1} = \sum_{i=1}^{d_1} \sum_{j=1}^{d_2} \sum_{l=1}^{d_3} |\mathcal{W}_{ijl} \mathcal{X}_{ijl}|. \quad (6)$$

Definition 6. (Gradient tensor) (Wang et al. 2023a) For a tensor $\mathcal{X} \in \mathbb{R}^{d_1 \times d_2 \times d_3}$, its gradient tensor along the k-th mode is defined as

$$\mathcal{G}_k := \nabla_k(\mathcal{X}) = \mathcal{X} \times_k \mathbf{D}_{n_k}, k = 1, 2, 3, \quad (7)$$

where \mathbf{D}_{n_k} is a row circulant matrix of $(-1, 1, 0, \dots, 0)$.

Definition 7. (*t-FGJP*) For a tensor $\mathcal{X} \in \mathbb{R}^{d_1 \times d_2 \times d_3}$, the proposed *t-FGJP* norm is defined as

$$\|\mathcal{X}\|_{\text{t-FGJP}} := \frac{1}{\gamma} \sum_{k \in \Gamma} \|\mathcal{G}_k\|_{G,\alpha,*}, \quad (8)$$

where Γ represents a priori set of directions along which \mathcal{X} equips both low-rankness and smoothness priors and $\gamma := \#\{\Gamma\}$ denotes the cardinality of Γ .

Proof to Proposition 1

We first recall the Proposition 1.

Proposition 1. In FGTNN, for our proposed $g_\alpha(x) = 2c \cdot \frac{|\alpha-2|}{\alpha} \left(\left(\frac{|x|/c}{|\alpha-2|} + 1 \right)^{\alpha/2} - 1 \right)$, there exists a convex conjugate function $\phi : \mathbb{R} \rightarrow \mathbb{R}$ which satisfied

$$g_\alpha(x) = \min_{w \in \mathbb{R}_+} (w|x| + \phi(w)), \quad (9)$$

and for fixed x , the minimum is reached at $w = \xi(x)$, which is defined as

$$w = \xi(x) = \begin{cases} 1, & \text{if } \alpha = 2 \\ 2c/(|x| + 2c), & \text{if } \alpha = 0 \\ \exp(-|x|/2c), & \text{if } \alpha = -\infty \\ \left(\frac{|x|/c}{|\alpha-2|} + 1 \right)^{\alpha/2-1}, & \text{otherwise.} \end{cases} \quad (10)$$

Proof. For the general loss function $G_\alpha(z)$ (Barron 2019)

$$G_\alpha(z) = \beta^2 \frac{|\alpha-2|}{\alpha} \left(\left(\frac{(z/\beta)^2}{|\alpha-2|} + 1 \right)^{\alpha/2} - 1 \right), \quad (11)$$

where $\alpha \in \mathbb{R}$ and $c > 0$. Notice that $G_\alpha(z)$ has three removable singularities at $\alpha = 0, \alpha = 2$ and its limit at $\alpha = -\infty$. Through simple limit operations, $G_\alpha(z)$ is denoted as

$$G_\alpha(z) = \begin{cases} \frac{1}{2}z^2, & \text{if } \alpha = 2 \\ \beta^2 \ln \left(\frac{1}{2} (z/\beta)^2 + 1 \right), & \text{if } \alpha = 0 \\ \beta^2 \left(1 - \exp \left(-\frac{1}{2} (z/\beta)^2 \right) \right), & \text{if } \alpha \rightarrow -\infty \\ \beta^2 \frac{|\alpha-2|}{\alpha} \left(\left(\frac{(z/\beta)^2}{|\alpha-2|} + 1 \right)^{\alpha/2} - 1 \right), & \text{otherwise.} \end{cases} \quad (12)$$

According to half-quadratic (HQ) theory (Geman and Yang 1995), there exists a convex function $\psi : \mathbb{R} \rightarrow \mathbb{R}$, which satisfies

$$G_\alpha(z) = \min_w \left\{ \frac{1}{2}wz^2 + \psi(w) \right\}, \quad (13)$$

where the minimum reach at $w = \eta(z)$, which is defined as

$$w = \eta(z) = \begin{cases} G''_\alpha(0^+), & \text{if } z = 0 \\ G'_\alpha(z)/z, & \text{if } z \neq 0, \end{cases} \quad (14)$$

according to Eq. (12), w satisfies

$$w = \begin{cases} 1, & \text{if } \alpha = 2 \\ 2\beta^2/(z^2 + 2\beta^2), & \text{if } \alpha = 0 \\ \exp \left(-\frac{1}{2} (z/\beta)^2 \right), & \text{if } \alpha \rightarrow -\infty \\ \left(\frac{(z/\beta)^2}{|\alpha-2|} + 1 \right)^{(\alpha/2-1)}, & \text{otherwise.} \end{cases} \quad (15)$$

Let $|x| = \frac{1}{2}z^2$ and $\beta = \sqrt{2c}$, we have $g_\alpha(x) = G_\alpha(z)$. It follows from Eq. (13) that

$$g_\alpha(x) = G_\alpha(z) = \min_w \left\{ \frac{1}{2}wz^2 + \psi(w) \right\} = \min_w \{w|x| + \psi(w)\}, \quad (16)$$

where the minimum is reached at $w = \eta(z) = \eta(\sqrt{2|x|})$. Therefore, we have

$$w = \eta(\sqrt{2|x|}) = \begin{cases} 1, & \text{if } \alpha = 2 \\ 2c/(|x| + 2c), & \text{if } \alpha = 0 \\ \exp(-|x|/2c), & \text{if } \alpha = -\infty \\ \left(\frac{|x|/c}{|\alpha-2|} + 1 \right)^{\alpha/2-1}, & \text{otherwise.} \end{cases} \quad (17)$$

This completes the proof. \square

Optimization for SFGTRPCA

We start by recalling the proposed SFGTRPCA model

$$\min_{\mathcal{L}, \mathcal{E}} \|\mathcal{L}\|_{\text{t-FGJP}} + \lambda \|\mathcal{E}\|_{G,\alpha,1} \text{ s.t. } \mathcal{M} = \mathcal{L} + \mathcal{E}. \quad (18)$$

According to Definition 7, we have

$$\|\mathcal{L}\|_{\text{t-FGJP}} := \frac{1}{\gamma} \sum_{k \in \Gamma} \|\mathcal{G}_k\|_{G,\alpha,*}. \quad (19)$$

For convenience, we ignore the subscript and transform $\|\mathcal{G}\|_{G,\alpha,*}$ into the following formula via Proposition 1

$$\|\mathcal{G}\|_{G,\alpha,*} = \min_{\mathbf{W}} \frac{1}{d_3} \sum_{j=1}^{d_3} \sum_{i=1}^d (W_{ji} \sigma_i(\bar{\mathbf{G}}^{(j)}) + \phi(W_{ji})), \quad (20)$$

where the W_{ji} is the (j, i) -th element of matrix $\mathbf{W} \in \mathbb{R}^{d_3 \times d}$. The minimum is reached at $W_{ji} = \xi(\sigma_i(\bar{\mathbf{G}}^{(j)}); c)$. Analogously, as for $\|\mathcal{E}\|_{G,\alpha,1}$, we have

$$\|\mathcal{E}\|_{G,\alpha,1} = \min_{\mathbf{W}} \sum_{i=1}^{d_1} \sum_{j=1}^{d_2} \sum_{l=1}^{d_3} (\mathcal{W}_{ijl} |\mathcal{E}_{ijl}| + \phi(\mathcal{W}_{ijl})), \quad (21)$$

where the \mathcal{W}_{ijl} is the (i, j, l) -th element of tensor $\mathcal{W} \in \mathbb{R}^{d_1 \times d_2 \times d_3}$. The minimum is reached at $\mathcal{W}_{ijk} = \xi(|\mathcal{E}_{ijk}|; c)$. Thus, by integrating Eq. (20), Eq. (21) and Eq. (19) into model (18), combining the definition of WTNN and WTLIN, the problem of SFGTRPCA can be reformulated as

$$\begin{aligned} & \min_{\mathcal{L}, \mathcal{G}_k, \mathcal{E}, \mathbf{W}_k, \mathcal{W}} \frac{1}{\gamma} \sum_{k \in \Gamma} (\|\mathcal{G}_k\|_{\mathbf{W},*} + \Phi_M(\mathbf{W}_k)) + \lambda \|\mathcal{E}\|_{\mathbf{W},1} \\ & + \Phi_T(\mathcal{W}) \text{ s.t. } \mathcal{M} = \mathcal{L} + \mathcal{E}, \mathcal{G}_k = \nabla_k(\mathcal{L}), \end{aligned} \quad (22)$$

where $\Phi_M(\mathbf{W})$ and $\Phi_T(\mathcal{W})$ are defined such that $(\Phi_M(\mathbf{W}))_{ji} = \phi(W_{ji})$ and $(\Phi_T(\mathcal{W}))_{ijl} = \phi(\mathcal{W}_{ijl})$. Then the Lagrangian function of the SFGTRPCA model is

$$\begin{aligned} L(\mathcal{L}, \mathcal{G}_k, \mathcal{E}, \mathbf{W}_k, \mathcal{W}, \mathcal{Y}_k, \mathcal{Z}, \mu) = & \sum_{k \in \Gamma} \left(\frac{1}{\gamma} \|\mathcal{G}_k\|_{\mathbf{W},*} + \right. \\ & \left. \frac{\mu}{2} \|\nabla_k(\mathcal{L}) - \mathcal{G}_k + \frac{\mathcal{Y}_k}{\mu}\|_F^2 - \frac{\mu}{2} \|\mathcal{Y}_k/\mu\|_F^2 + \frac{1}{\gamma} \Phi_M(\mathbf{W}_k) \right) + \end{aligned}$$

$$\lambda \|\mathcal{E}\|_{\mathcal{W},1} - \frac{\mu}{2} \|\mathcal{Z}/\mu\|_F^2 + \Phi_T(\mathcal{W}) + \frac{\mu}{2} \|\mathcal{M} - \mathcal{L} - \mathcal{E} + \frac{\mathcal{Z}}{\mu}\|_F^2, \quad (23)$$

where we consider $\Gamma = \{1, 2, 3\}$ here; \mathcal{Y}_k and \mathcal{Z} are Lagrange multipliers; μ is a positive parameter. Each variable can be updated alternately in the scheme of the ADMM framework.

Step1: Update \mathcal{L} by fixing the other variables:

$$\begin{aligned} \mathcal{L}_{t+1} = \arg \min_{\mathcal{L}} \sum_{k=1}^3 \left(\frac{\mu_t}{2} \|\nabla_k(\mathcal{L}) - \mathcal{G}_{k(t)} + \frac{\mathcal{Y}_{k(t)}}{\mu_t}\|_F^2 \right) + \\ \frac{\mu_t}{2} \|\mathcal{M} - \mathcal{L} - \mathcal{E}_t + \frac{\mathcal{Z}_t}{\mu_t}\|_F^2. \end{aligned} \quad (24)$$

By taking the \mathcal{L} derivative in Eq. (24), we can get the following equation that updates \mathcal{L}

$$\begin{aligned} (\mathcal{M} - \mathcal{E}_t + \mathcal{Z}_t/\mu_t + \sum_{k=1}^3 \nabla_k^T (\mathcal{G}_{k(t)} - \mathcal{Y}_{k(t)}/\mu_t)) \\ = (\mathcal{I} + \sum_{k=1}^3 \nabla_k^T \nabla_k)(\mathcal{L}), \end{aligned} \quad (25)$$

where $\nabla_k^T(\cdot)$ represents the transpose operator of $\nabla_k(\cdot)$ and \mathcal{I} is an identity tensor. In the Fourier domain, we can diagonalize the difference tensors \mathcal{D}_k corresponding to $\nabla_k^T(\cdot)$'s and apply the convolution theorem to derive the closed-form solution for updating \mathcal{L} in Eq. (25) (Wang et al. 2023a).

$$\mathcal{L}_{t+1} = \mathcal{F}^{-1} \left(\frac{\mathcal{F}(\mathcal{M} - \mathcal{E}_t + \mathcal{Z}_t/\mu_t) + \mathcal{H}}{1 + \sum_{k=1}^3 \mathcal{F}(\mathcal{D}_k)^* \odot \mathcal{F}(\mathcal{D}_k)} \right), \quad (26)$$

where $\mathcal{H} = \sum_{k=1}^3 \mathcal{F}(\mathcal{D}_k)^* \odot \mathcal{F}(\mathcal{G}_{k(t)} - \mathcal{Y}_{k(t)}/\mu_t)$, \mathcal{F} denotes the multi-dimensional FFT (Wang et al. 2008), and $\mathbf{1} \in \mathbb{R}^{d_1 \times d_2 \times d_3}$ denotes a tensor with all elements are 1, \odot is defined as an element-wise multiplication operator.

Step2: Update \mathcal{G}_k by fixing the other variables:

$$\begin{aligned} \mathcal{G}_{k(t+1)} = \arg \min_{\mathcal{G}_k} \frac{1}{3\mu_t} \|\mathcal{G}_k\|_{\mathcal{W},*} + \\ \frac{1}{2} \|\nabla_k(\mathcal{L}_{t+1}) - \mathcal{G}_k + \frac{\mathcal{Y}_{k(t)}}{\mu_t}\|_F^2. \end{aligned} \quad (27)$$

Therefore, we can update $\mathcal{G}_{k(t+1)}$ based on the proximal operator defined in the main paper.

$$\mathcal{G}_{k(t+1)} = \text{Prox}_{\|\cdot\|_{\frac{1}{3\mu_t} \mathcal{W},*}}(\nabla_k(\mathcal{L}_{t+1}) + \frac{\mathcal{Y}_{k(t)}}{\mu_t}) \quad (28)$$

Step3: Update \mathcal{E} by fixing the other variables:

$$\mathcal{E}_{t+1} = \arg \min_{\mathcal{E}} \frac{\lambda}{\mu_t} \|\mathcal{E}\|_{\mathcal{W},1} + \frac{1}{2} \|\mathcal{M} - \mathcal{L}_{t+1} - \mathcal{E} + \frac{\mathcal{Z}_t}{\mu_t}\|_F^2. \quad (29)$$

By using the TST operator defined in the main paper, we can update \mathcal{E}_t by

$$\mathcal{E}_{t+1} = \text{TST}(\mathcal{M} - \mathcal{L}_{t+1} + \mathcal{Z}_t/\mu_t, \frac{\lambda}{\mu_t} \mathcal{W}_t). \quad (30)$$

Algorithm 1: SFGTRPCA algorithm

Input: Observation tensor data $\mathcal{M} \in \mathbb{R}^{d_1 \times d_2 \times d_3}$, and the parameter $\lambda, \rho = 1.25, \epsilon = 10^{-6}$.

- 1: Initialize $\mathcal{L}_0 = \mathcal{G}_{k(0)} = \mathcal{Y}_{k(0)} = \mathcal{E}_0 = \mathcal{Z}_0 = 0$, $\mathbf{W}_{k(0)} = \mathbf{1}_{d_3 \times d}$, $\mathcal{W}_0 = \mathbf{1}_{d_1 \times d_2 \times d_3}$, $\mu_0 = 10^{-4}$, and $t = 0$.
- 2: **while** not converge **do**
- 3: Update the low-rank tensor \mathcal{L} by Eq. (26).
- 4: Update the gradient tensor \mathcal{G}_k by Eq. (28).
- 5: Update the sparse tensor \mathcal{E} by Eq. (30).
- 6: Update the weights \mathbf{W}_k and \mathcal{W} by Eq. (31).
- 7: Update the Lagrangian multipliers \mathcal{Y}_k and \mathcal{Z} by Eq. (32) and Eq. (33), respectively.
- 8: Update the parameter μ by Eq. (34).
- 9: Check the convergence condition in Eq. (35).
- 10: **end while**

Output: $\mathcal{L} = \mathcal{L}_{t+1}, \mathcal{E} = \mathcal{E}_{t+1}$

Step4: Update the elements of \mathbf{W}_k and \mathcal{W} by an adaptive way according to Proposition 1

$$W_{k(t+1)ji} = \xi(\sigma_i(\bar{\mathbf{G}}_{k(t+1)}^{(j)}; c), \mathcal{W}_{(t+1)ijl} = \xi(|(\mathcal{E}_{t+1})_{ijl}|; c). \quad (31)$$

Step5: Update the Lagrangian multiplier tensor \mathcal{Y}_k and \mathcal{Z} , as well as the parameter μ by

$$\mathcal{Y}_{k(t+1)} = \mathcal{Y}_{k(t)} + \mu_t(\nabla_k(\mathcal{L}_{t+1}) - \mathcal{G}_{k(t+1)}), \quad (32)$$

$$\mathcal{Z}_{t+1} = \mathcal{Z}_t + \mu_t(\mathcal{M} - \mathcal{L}_{t+1} - \mathcal{E}_{t+1}), \quad (33)$$

$$\mu_{t+1} = \rho \mu_t, \quad (34)$$

where $\rho = 1.25$. The convergence conditions are defined as

$$\left\{ \begin{array}{l} \|\mathcal{L}_{t+1} - \mathcal{L}_t\|_\infty \\ \|\mathcal{E}_{t+1} - \mathcal{E}_t\|_\infty \\ \|\mathcal{M} - \mathcal{L}_{t+1} - \mathcal{E}_{t+1}\|_\infty \end{array} \right\} \leq \epsilon, \quad (35)$$

The whole optimization procedure is summarized in Algorithm 1.

Additional Experiments

In this section, we provide several additional experimental results that further validate the effectiveness of our proposed models.

Settings

Datasets: For comprehensive comparison, we use 4 widely used tensor data types including color images, grayscale videos, hyperspectral images (HSIs), and multispectral images (MSIs). For color images, we choose 3 widely used datasets including Berkeley Segmentation Dataset¹ (BSD) (Martin et al. 2001), Kodak (Kodak 1993) dataset², and ZheJiang University (ZJU) (Hu et al. 2012) dataset³. For grayscale videos, we use 14 grayscale video sequences from the YUV dataset⁴ and select the first 100 frames for each sequence. For HSIs, we select Cuprite⁵, DCMall⁵, Urban⁵, In-

¹<https://www2.eecs.berkeley.edu/Research/Projects/CS/vision/bbsd/>

²<http://r0k.us/graphics/kodak/>

³<https://sites.google.com/site/zjuyaohu/>

⁴<http://trace.eas.asu.edu/yuv/>

⁵<https://lesun.weebly.com/hyperspectral-data-set.html>

	Noise Ratio	10%		20%		30%	
		Methods	τ^L	τ^E	τ^L	τ^E	τ^L
CIs.	FGTRPCA	0.5	10	1	5	0.5	1
	SFGTRPCA	0.1	5	0.1	1	0.1	0.5
GVs.	FGTRPCA	0.5	5	0.5	1	0.5	0.5
	SFGTRPCA	0.1	4	0.1	1	0.5	0.5
HSIs	FGTRPCA	0.5	5	1	1	3	5
	SFGTRPCA	0.1	1	0.1	1	0.5	0.5
MSIs	FGTRPCA	0.5	50	1	5	3	5
	SFGTRPCA	0.1	5	0.1	1	0.5	0.1

Table 2: Parameter selection for τ^L and τ^E used in FGTRPCA and SFGTRPCA methods. CIs. and GVs. represent the color images and grayscale videos.

dian Pines⁵, and Pavia University⁵ (PaviaU) for experiments and select the first 50 bands from each HSI dataset. For MSIs, we randomly select 10 MSIs from the CAVE dataset (Yasuma et al. 2008).

Baselines: Our baselines are divided into two categories based on different priors. (1) Low-rankness: TRPCA (Lu et al. 2020), ETRPCA (Gao et al. 2020), and PTRPCA (Yan and Guo 2024); (2) Joint Low-rankness & Smoothness: t-CTV (Wang et al. 2023a) and RTCTV (Huang et al. 2024).

Parameter selection: We utilize the parameters recommended by the corresponding authors. For our FGTRPCA and SFGTRPCA, there are three parameters: α , c^L for low-rank regularize, and c_E for sparse regularizer. We set $\alpha = 1$ throughout the paper; c_L and c_E can be estimated adaptively in a median form, i.e.,

$$c_j^L = \tau^L \times \text{mean}(\sigma_1(\bar{\mathbf{L}}^{(j)}), \dots, \sigma_d(\bar{\mathbf{L}}^{(j)})), \quad (36)$$

$$c^E = \tau^E \times \text{mean}(|\mathcal{E}_{ijk}|, (i, j, k) \in [d_1] \times [d_2] \times [d_3]), \quad (37)$$

where $\bar{\mathbf{L}}^{(j)}$ is the j -th frontal slice of the low-rank tensor \mathcal{L} , and all the singular values of $\bar{\mathbf{L}}^{(j)}$ sharing the same parameter c_j^L ; \mathcal{E}_{ijl} is the (i, j, l) -th entry of the sparse tensor \mathcal{E} and $(i, j, l) \in [d_1] \times [d_2] \times [d_3]$ means $i = 1, 2, \dots, d_1, j = 1, 2, \dots, d_2, l = 1, 2, \dots, d_3$. τ^L and τ^E used in various tensor denoising tasks are summarized in Table 2, and the values in some datasets are slightly adjusted.

Evaluation metrics: The peak signal-to-noise ratio (PSNR), structural similarity (SSIM), and feature similarity (FSIM) are employed to evaluate the recovery performance for color images and grayscale videos. For HSIs and MSIs, we adopt the PSNR, SSIM, and Erreur Relative Globale Adimensionnelle de Synthese (ERGAS) for evaluation.

Results

Visual Quality. In the main text, we provide a visual comparison of the performance of various algorithms in color image recovery, highlighting the advantages of our proposed method. In this supplementary material, we extend our analysis by presenting the recovery results on additional visual

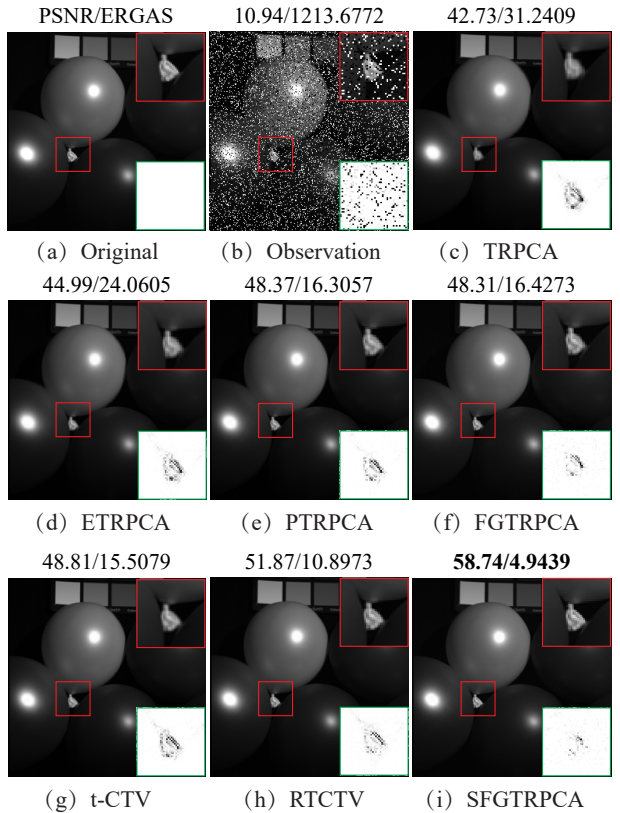


Figure 1: Recovery performance comparison of all methods on the 40-th band on MSI ‘balloons’ dataset with 20% noise.

datasets, further demonstrating the effectiveness of our approach across different types of data compared to other algorithms. In Figure 1, 2 and 4, the recovery performance of various methods across different datasets is visually presented. It is evident that our proposed SFGTRPCA demonstrates significant advantages in various scenarios. Notably, for datasets with clear smoothness in the spectral direction (HSIs and MSIs), methods that simultaneously account for low-rankness and smoothness priors perform better. Conversely, for datasets where spectral direction smoothness is less pronounced (grayscale videos and color images), our proposed FGTRPCA also exhibits superior performance. This highlights the superiority of our proposed FGTNN and underscores the importance of its adaptability to different prior data types.

Quantitative Quality. In the main paper, we demonstrate the recovery performance of various methods under noise levels of 10% and 20%, evaluating their effectiveness on different types of data using PSNR and SSIM metrics. This supplementary material provides a more detailed and visual comparison of the performances of all methods. We also increase the noise levels to challenge the algorithms further and assess their performance in more complex scenarios. The detailed results are shown in Table 4, 5, 6, and 7.

Methods		TRPCA	ETRPCA	PTRPCA	FGTRPCA	t-CTV	RTCTV	SFGTRPCA
TRPCA	h	-	1	1	1	1	1	1
	p		2.21E-80	5.93E-85	1.56E-93	6.86E-85	2.31E-94	7.56E-88
ETRPCA	h	1	-	1	1	1	1	1
	p	2.21E-80		2.69E-79	5.46E-95	6.31E-70	2.01E-86	2.79E-81
PTRPCA	h	1	1	-	1	1	1	1
	p	5.93E-85	2.69E-79		1.91E-98	2.51E-74	2.00E-19	1.87E-26
FGTRPCA	h	1	1	1	-	1	1	1
	p	1.56e-93	5.46E-95	1.91E-98		4.56E-96	5.19E-98	1.33E-97
t-CTV	h	1	1	1	1	-	1	1
	p	6.86E-85	6.31E-70	2.51E-74	4.56E-96		6.63E-84	1.28E-80
RTCTV	h	1	1	1	1	1	-	1
	p	2.31E-94	2.01E-86	2.00E-19	5.19E-98	6.63E-84		1.94E-05
SFGTRPCA	h	1	1	1	1	1	1	-
	p	7.56E-88	2.79E-81	1.87E-26	1.33E-97	1.28E-80	1.943E-05	

Table 3: The t-test results pertain to the average relative recovery error of various TRPCA methods over 50 runs. Here, h represents the test decision for the null hypothesis, which posits that the difference in relative recovery errors between the two methods follows a normal distribution with a mean of zero and an unknown variance. The paired-sample t-test was used for this analysis. A result of $h = 1$ indicates that the test rejects the null hypothesis at the 5% significance level, while $h = 0$ indicates that the null hypothesis is not rejected. The variable p denotes the p -value associated with the t-test.

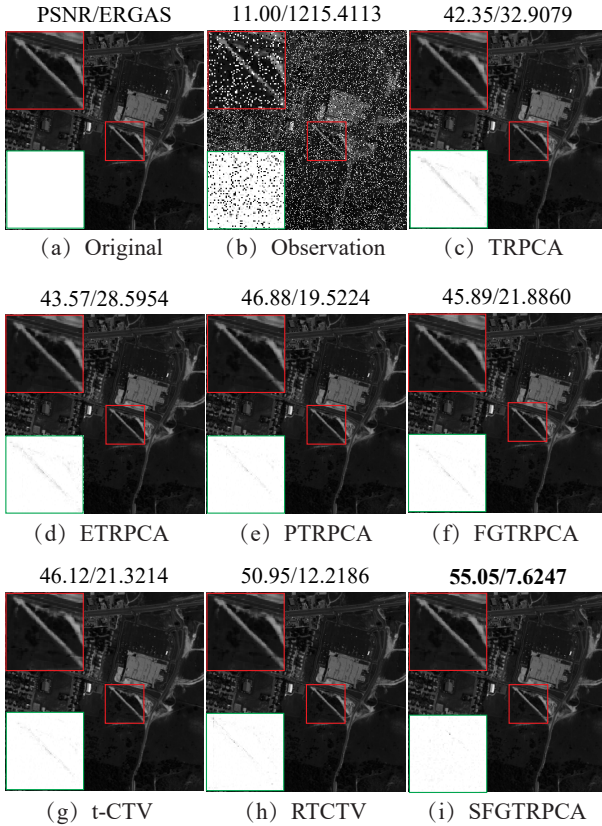


Figure 2: Recovery performance comparison of all methods on the 40-th band on HSI ‘Urban’ dataset with 20% noise.

Convergence Analysis

The convergence of our proposed FGTRPCA and SFGTRPCA algorithms is evaluated through experiments on color

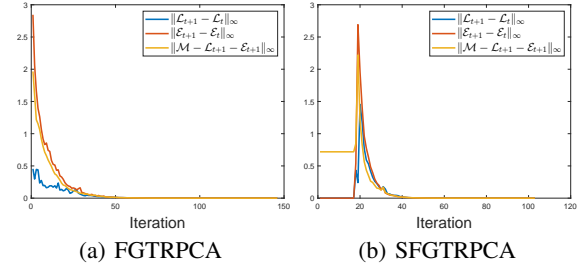


Figure 3: The convergence behavior of FGTRPCA and SFGTRPCA algorithms.

image recovery by using a sample from the BSD dataset, which is corrupted with 10% noise. Specifically, we take the top convergence criterion from both algorithms as functions of errors versus the number of iterations. As seen in Fig. 3, The errors reach zero with 50 iterations, which means good convergence of our proposed algorithms in practice.

t-test

In this experiment, we conduct a series of t-tests to evaluate the statistical significance of the differences between any two methods. The primary objective is to determine whether the observed differences in their results are statistically significant. Each method is applied to the datasets, and the resulting performance metrics are recorded. The null hypothesis for each t-test is that there is no significant difference between the two methods being compared. A significance level of 0.05 is used to assess the p -values, and any p -value below this threshold indicates a statistically significant difference between the methods. The results are presented in Table 3. As observed, the p -values for comparisons between any two methods are close to 0 and all below 0.05. This indicates a significant difference between the proposed FGTR-

PCA, SFGTRPCA, and the other competing methods, as confirmed by the t-test.

References

- Barron, J. T. 2019. A general and adaptive robust loss function. In *Proceedings of the IEEE/CVF conference on computer vision and pattern recognition*, 4331–4339.
- Gao, Q.; Zhang, P.; Xia, W.; Xie, D.; Gao, X.; and Tao, D. 2020. Enhanced tensor RPCA and its application. *IEEE Transactions on Pattern Analysis and Machine Intelligence*, 43(6): 2133–2140.
- Geman, D.; and Yang, C. 1995. Nonlinear image recovery with half-quadratic regularization. *IEEE Transactions on Image Processing*, 4(7): 932–946.
- Hu, Y.; Zhang, D.; Ye, J.; Li, X.; and He, X. 2012. Fast and accurate matrix completion via truncated nuclear norm regularization. *IEEE Transactions on Pattern Analysis and Machine Intelligence*, 35(9): 2117–2130.
- Huang, K.; Kong, W.; Zhou, M.; Qin, W.; Zhang, F.; and Wang, J. 2024. Enhanced Low-Rank Tensor Recovery Fusing Reweighted Tensor Correlated Total Variation Regularization for Image Denoising. *Journal of Scientific Computing*, 99(3): 69.
- Kilmer, M.; and Martin, C. 2011. Factorization strategies for third-order tensors. *Linear Algebra Appl.*, 435(3): 641–658.
- Kodak. E. 1993. Kodak lossless true color image suite (PhotoCD PCD0992). URL <http://r0k.us/graphics/kodak>, 6: 2.
- Lu, C.; Feng, J.; Chen, Y.; Liu, W.; Lin, Z.; and Yan, S. 2020. Tensor Robust Principal Component Analysis with a New Tensor Nuclear Norm. *IEEE Transactions on Pattern Analysis and Machine Intelligence*, 42(4): 925–938.
- Martin, D.; Fowlkes, C.; Tal, D.; and Malik, J. 2001. A database of human segmented natural images and its application to evaluating segmentation algorithms and measuring ecological statistics. In *Proceedings eighth IEEE international conference on computer vision. ICCV2001*, volume 2, 416–423. IEEE.
- Wang, H.; Peng, J.; Qin, W.; Wang, J.; and Meng, D. 2023a. Guaranteed tensor recovery fused low-rankness and smoothness. *IEEE Transactions on Pattern Analysis and Machine Intelligence*, 45(9): 10990–11007.
- Wang, Y.; Kou, K. I.; Chen, H.; Tang, Y. Y.; and Li, L. 2023b. Double Auto-Weighted Tensor Robust Principal Component Analysis. *IEEE Transactions on Image Processing*, 32: 5114–5125.
- Wang, Y.; Yang, J.; Yin, W.; and Zhang, Y. 2008. A new alternating minimization algorithm for total variation image reconstruction. *SIAM Journal on Imaging Sciences*, 1(3): 248–272.
- Yan, T.; and Guo, Q. 2024. Tensor robust principal component analysis via dual l_p quasi-norm sparse constraints. *Digital Signal Processing*, 150: 104520.
- Yasuma, F.; Mitsunaga, T.; Iso, D.; and Nayar, S. K. 2008. Generalized Assorted Pixel Camera: Post-Capture Control of. *Tech. rep., Department of Computer Science, Columbia University CUCS-061-08*.



Figure 4: Comparison of recovery performance across all methods on the grayscale video sequences of akiyo, coastguard, and salesman. The 30-th frame of each sequence is displayed.

Dataset	Noise Ratio	10%			20%			30%			
		Methods	PSNR↑	SSIM↑	FSIM↑	PSNR↑	SSIM↑	FSIM↑	PSNR↑	SSIM↑	FSIM↑
BSD	FGTRPCA	TRPCA	29.62	0.9385	0.9467	27.95	0.8979	0.9227	26.30	0.8273	0.8907
		ETRPCA	32.80	0.9608	0.9705	30.40	0.9184	0.9483	26.64	0.8159	0.8903
		PTRPCA	31.78	0.9578	0.9666	29.86	0.9257	0.9477	27.93	0.8654	0.9189
		<u>35.79</u>	<u>0.9755</u>	<u>0.9845</u>	31.92	0.9387	0.9460	28.90	0.8626	0.9286	
		TCTV	31.29	0.9442	0.9604	30.16	0.9232	0.9472	29.05	0.8955	0.9307
		RTCTV	33.62	0.9649	0.9761	32.07	0.9458	0.9648	30.43	0.9106	0.9463
Kodak	SFGTRPCA	39.66	0.9896	0.9937	<u>35.39</u>	<u>0.9720</u>	<u>0.9836</u>	<u>32.42</u>	<u>0.9410</u>	<u>0.9671</u>	
		TRPCA	29.63	0.9323	0.9651	28.26	0.8946	0.9517	26.89	0.8317	0.9334
		ETRPCA	32.48	0.9523	0.9820	30.65	0.9155	0.9721	27.18	0.7673	0.9418
		PTRPCA	31.25	0.9480	0.9780	29.76	0.9170	0.9680	28.32	0.8693	0.9539
		<u>35.74</u>	<u>0.9744</u>	<u>0.9929</u>	32.23	0.9143	0.9822	29.10	0.8873	0.9662	
		TCTV	31.69	0.9412	0.9847	30.69	0.9209	0.9792	29.71	0.8946	0.9715
ZJU	SFGTRPCA	RTCTV	33.96	0.9612	0.9907	32.60	0.9428	0.9862	31.13	0.9066	0.9771
		39.47	0.9874	0.9972	<u>35.76</u>	<u>0.9777</u>	<u>0.9877</u>	<u>33.04</u>	<u>0.9415</u>	<u>0.9860</u>	
		TRPCA	34.37	0.9685	0.9730	32.44	0.9419	0.9576	30.27	0.8812	0.9339
		ETRPCA	34.49	0.9610	0.9723	32.65	0.9361	0.9578	30.81	0.8837	0.9369
		PTRPCA	37.07	0.9809	0.9853	34.67	0.9624	0.9739	32.19	0.9149	0.9527
		40.26	0.9889	0.9927	35.64	0.9714	0.9804	33.35	0.9423	0.9647	
DC Mall	SFGTRPCA	TCTV	35.54	0.9722	0.9807	34.27	0.9603	0.9729	32.86	0.9426	0.9621
		RTCTV	37.34	0.9809	0.9872	35.73	0.9703	0.9807	33.82	0.9435	0.9669
		43.77	0.9951	0.9968	<u>39.66</u>	<u>0.9850</u>	<u>0.9909</u>	<u>36.43</u>	<u>0.9713</u>	<u>0.9825</u>	

Table 4: Quantitative comparisons of color images with different noise ratios. Best results are marked bold and second-best results are underlined.

Dataset	Noise Ratio	10%			20%			30%			
		Methods	PSNR↑	SSIM↑	ERGAS↓	PSNR↑	SSIM↑	ERGAS↓	PSNR↑	SSIM↑	ERGAS↓
Cuprite	FGTRPCA	TRPCA	54.85	0.9948	23.29	52.07	0.9937	25.26	48.96	0.9918	27.46
		ETRPCA	54.07	0.9942	22.20	52.16	0.9932	23.79	50.04	0.9917	25.52
		PTRPCA	58.78	0.9961	18.09	56.20	0.9954	19.56	53.28	0.9942	21.04
		<u>59.56</u>	<u>0.9976</u>	<u>11.59</u>	<u>56.46</u>	<u>0.9967</u>	<u>13.33</u>	<u>52.94</u>	<u>0.9953</u>	<u>15.75</u>	
		t-CTV	56.72	0.9961	17.29	54.85	0.9956	18.39	52.68	0.9947	19.43
		RTCTV	56.41	0.9954	15.70	55.08	0.9950	16.36	53.78	0.9947	19.12
DC Mall	SFGTRPCA	62.68	0.9983	10.02	<u>60.38</u>	<u>0.9976</u>	<u>12.93</u>	<u>58.47</u>	<u>0.9971</u>	<u>13.63</u>	
		TRPCA	44.96	0.9834	65.25	42.81	0.9811	70.76	39.95	0.9775	78.02
		ETRPCA	45.75	0.9853	56.65	43.86	0.9833	61.21	41.58	0.9807	66.37
		PTRPCA	49.33	0.9884	50.47	46.54	0.9865	55.25	42.15	0.9829	61.19
		47.92	<u>0.9933</u>	<u>34.19</u>	<u>44.74</u>	<u>0.9873</u>	<u>49.85</u>	<u>41.55</u>	<u>0.9827</u>	<u>61.72</u>	
		t-CTV	46.68	0.9887	46.53	44.55	0.9873	49.93	<u>44.32</u>	<u>0.9875</u>	<u>48.02</u>
Urban	SFGTRPCA	RTCTV	50.32	0.9926	33.11	47.22	0.9926	40.98	42.12	0.9854	54.14
		54.54	0.9953	<u>29.32</u>	<u>51.78</u>	<u>0.9938</u>	<u>34.06</u>	<u>46.22</u>	<u>0.9914</u>	<u>39.17</u>	
		TRPCA	46.98	0.9951	34.47	45.29	0.9937	38.73	43.12	0.9907	44.85
		ETRPCA	47.70	0.9947	32.30	46.42	0.9936	35.32	44.64	0.9916	39.77
		PTRPCA	50.29	0.9967	25.90	48.86	0.9958	28.66	46.70	0.9940	32.86
		49.60	<u>0.9972</u>	<u>21.71</u>	<u>47.16</u>	<u>0.9952</u>	<u>29.12</u>	<u>44.76</u>	<u>0.9923</u>	<u>36.58</u>	
Indain Pines	SFGTRPCA	t-CTV	48.94	0.9964	25.64	47.56	0.9956	28.13	45.96	0.9944	31.54
		RTCTV	52.97	0.9968	20.46	52.14	0.9964	21.56	<u>48.57</u>	<u>0.9954</u>	<u>27.49</u>
		58.87	0.9989	<u>12.29</u>	<u>55.40</u>	<u>0.9983</u>	<u>14.62</u>	<u>53.20</u>	<u>0.9972</u>	<u>19.94</u>	
		TRPCA	35.55	0.9320	69.89	34.68	0.9229	72.58	33.27	0.8976	77.94
		ETRPCA	35.91	0.9315	67.64	35.19	0.9250	69.13	32.60	0.8686	78.41
		PTRPCA	37.66	0.9490	59.20	36.10	0.9355	61.09	30.27	0.7835	95.16
PaviaU	SFGTRPCA	38.77	<u>0.9587</u>	<u>51.10</u>	<u>37.03</u>	<u>0.9443</u>	<u>57.38</u>	<u>35.51</u>	<u>0.9279</u>	<u>64.26</u>	
		t-CTV	36.50	0.9356	64.96	35.98	0.9312	66.30	35.30	0.9245	68.41
		RTCTV	37.89	0.9448	57.67	36.37	0.9356	57.38	<u>35.78</u>	<u>0.9284</u>	<u>65.35</u>
		40.43	0.9640	<u>47.74</u>	<u>39.00</u>	<u>0.9553</u>	<u>50.95</u>	<u>37.15</u>	<u>0.9419</u>	<u>57.34</u>	
		TRPCA	38.59	0.9718	63.04	37.55	0.9677	68.64	36.45	0.9619	75.46
		ETRPCA	39.29	0.9679	60.92	38.37	0.9646	65.27	37.28	0.9599	71.01
PaviaU	SFGTRPCA	PTRPCA	40.83	0.9771	52.73	39.71	0.9730	57.54	38.39	0.9674	63.74
		40.69	<u>0.9825</u>	<u>47.60</u>	<u>39.13</u>	<u>0.9703</u>	<u>56.53</u>	<u>37.68</u>	<u>0.9622</u>	<u>66.33</u>	
		t-CTV	39.80	0.9729	55.42	39.03	0.9702	59.03	38.25	0.9668	63.04
		RTCTV	43.85	0.9766	42.18	43.00	0.9748	44.31	40.03	0.9700	<u>55.49</u>
		45.42	0.9876	<u>34.47</u>	<u>44.28</u>	<u>0.9834</u>	<u>37.32</u>	<u>42.18</u>	<u>0.9767</u>	<u>44.26</u>	

Table 5: Quantitative comparisons of HSIs with different noise ratios. Best results are marked bold and second-best results are underlined.

Dataset	Noise Ratio Methods	10%			20%			30%		
		PSNR↑	SSIM↑	FSIM↑	PSNR↑	SSIM↑	FSIM↑	PSNR↑	SSIM↑	FSIM↑
Akiyo	TRPCA	38.03	0.9859	0.9897	37.00	0.9826	0.9875	35.90	0.9784	0.9846
	ETRPCA	41.70	0.9922	0.9942	40.40	0.9903	0.9929	37.68	0.9841	0.9885
	PTRPCA	42.81	0.9939	0.9954	41.32	0.9922	0.9942	39.76	0.9895	0.9926
	FGTRPCA	<u>46.25</u>	0.9968	0.9974	43.79	0.9949	0.9960	<u>41.08</u>	0.9921	0.9940
	t-CTV	40.77	0.9912	0.9938	39.84	0.9896	0.9927	38.73	0.9874	0.9911
	RTCTV	45.74	0.9955	0.9967	44.75	0.9949	0.9962	40.14	0.9898	0.9928
Carphone	SFGTRPCA	50.92	0.9982	0.9987	48.00	0.9970	0.9980	45.54	0.9957	0.9971
	TRPCA	32.58	0.9549	0.9655	31.86	0.9454	0.9599	31.02	0.9283	0.9516
	ETRPCA	35.14	0.9703	0.9782	33.77	0.9413	0.9663	32.09	0.9243	0.9549
	PTRPCA	35.49	0.9742	0.9810	34.40	0.9595	0.9742	32.00	0.8885	0.9445
	FGTRPCA	<u>37.52</u>	0.9760	0.9856	35.17	0.9521	0.9739	33.65	0.9424	0.9669
	t-CTV	34.33	0.9658	0.9739	33.75	0.9610	0.9707	33.17	0.9551	0.9669
Claire	RTCTV	37.45	0.9790	0.9850	35.26	0.9426	0.9685	34.04	0.9592	0.9709
	SFGTRPCA	39.79	0.9864	0.9913	37.78	0.9782	0.9862	36.22	0.9675	0.9798
	TRPCA	39.18	0.9878	0.9898	37.96	0.9848	0.9873	36.94	0.9811	0.9844
	ETRPCA	42.94	0.9924	0.9942	41.47	0.9903	0.9928	38.71	0.9853	0.9883
	PTRPCA	44.17	0.9939	0.9953	42.45	0.9919	0.9940	40.73	0.9885	0.9920
	FGTRPCA	<u>48.48</u>	0.9964	0.9975	45.01	0.9943	0.9959	42.59	0.9905	0.9937
Coastguard	t-CTV	41.78	0.9920	0.9942	40.88	0.9870	0.9931	39.94	0.9890	0.9918
	RTCTV	46.09	0.9946	0.9965	45.06	0.9939	0.9959	41.01	0.9903	0.9929
	SFGTRPCA	51.31	0.9978	0.9986	47.99	0.9963	0.9977	45.73	0.9947	0.9966
	TRPCA	30.56	0.9181	0.9377	29.44	0.8920	0.9260	27.99	0.8414	0.9091
	ETRPCA	33.39	0.9449	0.9654	28.20	0.8068	0.9295	25.80	0.6969	0.8949
	PTRPCA	34.10	0.9544	0.9691	31.02	0.9022	0.9522	28.81	0.8676	0.9236
Container	FGTRPCA	<u>35.67</u>	0.9651	0.9769	32.77	0.9367	0.9612	30.59	0.9026	0.9422
	t-CTV	31.34	0.9227	0.9465	30.53	0.9070	0.9381	29.74	0.8875	0.9290
	RTCTV	35.25	0.9609	0.9777	28.55	0.8093	0.9326	30.48	0.8965	0.9411
	SFGTRPCA	36.77	0.9749	0.9835	34.13	0.9545	0.9723	32.13	0.9332	0.9579
	TRPCA	41.71	0.9913	0.9937	40.34	0.9888	0.9923	38.20	0.9839	0.9900
	ETRPCA	45.69	0.9935	0.9957	44.16	0.9912	0.9948	41.32	0.9862	0.9923
Foreman	PTRPCA	46.48	0.9948	0.9963	44.98	0.9928	0.9954	43.05	0.9888	0.9940
	FGTRPCA	<u>49.40</u>	0.9961	0.9975	46.69	0.9946	0.9964	<u>44.54</u>	0.9907	0.9951
	t-CTV	43.94	0.9931	0.9956	42.41	0.9921	0.9948	40.81	0.9891	0.9936
	RTCTV	48.16	0.9943	0.9969	46.95	0.9935	0.9966	43.17	0.9906	0.9947
	SFGTRPCA	52.08	0.9977	0.9986	49.71	0.9966	0.9980	46.97	0.9951	0.9972
	TRPCA	31.65	0.9450	0.9504	30.36	0.9230	0.9370	28.93	0.8767	0.9164
Hall	ETRPCA	35.52	0.9661	0.9742	31.12	0.8550	0.9323	27.55	0.7188	0.8743
	PTRPCA	36.34	0.9731	0.9793	33.72	0.9344	0.9620	25.44	0.6253	0.8349
	FGTRPCA	<u>38.42</u>	0.9783	0.9854	<u>35.03</u>	0.9520	0.9720	32.20	0.9303	0.9523
	t-CTV	33.77	0.9606	0.9626	32.67	0.9517	0.9544	31.62	0.9345	0.9441
	RTCTV	<u>38.53</u>	0.9786	0.9843	31.94	0.8596	0.9347	<u>32.78</u>	0.9343	0.9516
	SFGTRPCA	41.23	0.9869	0.9915	37.97	0.9755	0.9831	35.26	0.9582	0.9702
Miss-america	TRPCA	34.00	0.9655	0.9702	33.30	0.9603	0.9729	32.53	0.9688	0.9753
	ETRPCA	36.32	0.9844	0.9866	35.46	0.9793	0.9843	34.08	0.9736	0.9795
	PTRPCA	36.50	0.9857	0.9876	35.59	0.9815	0.9853	34.70	0.9746	0.9822
	FGTRPCA	<u>40.58</u>	0.9892	0.9928	38.18	0.9787	0.9876	35.97	0.9807	0.9851
	t-CTV	36.81	0.9768	0.9833	36.29	0.9738	0.9816	35.65	0.9802	0.9835
	RTCTV	39.22	0.9886	0.9911	39.23	0.9878	0.9908	36.39	0.9818	0.9851
Mobile	SFGTRPCA	43.16	0.9937	0.9954	40.82	0.9879	0.9922	39.09	0.9872	0.9910
	TRPCA	38.64	0.9784	0.9792	37.54	0.9729	0.9746	36.35	0.9641	0.9683
	ETRPCA	42.04	0.9864	0.9882	40.47	0.9802	0.9842	38.05	0.9704	0.9750
	PTRPCA	43.06	0.9893	0.9907	41.31	0.9841	0.9871	39.53	0.9736	0.9813
	FGTRPCA	<u>46.49</u>	0.9934	0.9952	43.49	0.9885	0.9916	<u>41.01</u>	0.9782	0.9856
	t-CTV	41.43	0.9851	0.9876	40.60	0.9826	0.9853	39.75	0.9794	0.9827
Mother-daughter	RTCTV	44.63	0.9893	0.9922	<u>43.79</u>	0.9874	0.9909	40.61	0.9811	0.9846
	SFGTRPCA	49.20	0.9957	0.9973	46.57	0.9926	0.9953	44.52	0.9890	0.9929
	TRPCA	28.66	0.9472	0.9680	27.02	0.9205	0.9537	25.22	0.8668	0.9252
	ETRPCA	32.93	0.9719	0.9821	26.20	0.8564	0.9220	20.36	0.6351	0.8252
	PTRPCA	33.10	0.9740	0.9835	29.92	0.9399	0.9635	25.95	0.8890	0.9380
	FGTRPCA	<u>34.39</u>	0.9760	0.9842	<u>30.37</u>	0.9551	0.9736	27.88	0.9123	0.9501
News	t-CTV	29.59	0.9543	0.9745	28.18	0.9366	0.9652	26.78	0.9103	0.9512
	RTCTV	<u>35.61</u>	0.9808	0.9869	26.34	0.8579	0.9186	<u>27.91</u>	0.9130	0.9490
	SFGTRPCA	37.26	0.9871	0.9907	33.38	0.9737	0.9826	30.24	0.9463	0.9669
	TRPCA	39.18	0.9729	0.9811	38.01	0.9667	0.9772	36.81	0.9576	0.9721
	ETRPCA	41.52	0.9810	0.9876	40.01	0.9746	0.9845	37.87	0.9622	0.9765
	PTRPCA	42.52	0.9844	0.9898	40.99	0.9794	0.9873	38.32	0.9600	0.9792
Mother-daughter	FGTRPCA	<u>44.62</u>	0.9898	0.9938	42.29	0.9840	0.9903	<u>40.28</u>	0.9769	0.9859
	t-CTV	41.25	0.9795	0.9867	40.37	0.9762	0.9847	39.43	0.9717	0.9819
	RTCTV	43.61	0.9851	0.9912	42.64	0.9828	0.9903	40.08	0.9740	0.9839
	SFGTRPCA	47.52	0.9937	0.9966	45.23	0.9901	0.9946	43.50	0.9861	0.9922
	TRPCA	33.70	0.9667	0.9760	32.97	0.9616	0.9726	32.16	0.9549	0.9681
	ETRPCA	36.41	0.9796	0.9851	35.58	0.9758	0.9827	33.70	0.9643	0.9752
Salesman	PTRPCA	36.61	0.9812	0.9862	35.68	0.9769	0.9836	34.84	0.9710	0.9804
	FGTRPCA	<u>40.15</u>	0.9880	0.9923	38.03	0.9834	0.9892	35.87	0.9763	0.9843
	t-CTV	36.50	0.9802	0.9854	35.90	0.9775	0.9836	35.19	0.9740	0.9812
	RTCTV	39.98	0.9891	0.9920	39.63	0.9860	0.9909	36.33	0.9786	0.9845
	SFGTRPCA	42.83	0.9940	0.9956	41.19	0.9906	0.9938	39.17	0.9874	0.9914
	TRPCA	37.81	0.9761	0.9817	36.90	0.9718	0.9785	35.89	0.9662	0.9744
Silent	ETRPCA	40.49	0.9847	0.9886	39.44	0.9815	0.9865	37.20	0.9725	0.9796
	PTRPCA	41.25	0.9869	0.9903	40.10	0.9839	0.9883	38.70	0.9789	0.9850
	FGTRPCA	<u>44.77</u>	0.9934	0.9951	42.08	0.9891	0.9921	<u>40.16</u>	0.9841	0.9888
	t-CTV	40.06	0.9834	0.9875	39.29	0.9811	0.9858	38.48	0.9781	0.9835
	RTCTV	43.06	0.9897	0.9925	42.35	0.9888	0.9918	39.37	0.9810	0.9859
	SFGTRPCA	47.20	0.9955	0.9968	44.86	0.9931	0.9951	42.89	0.9902	0.9932
Suzie	TRPCA	34.00	0.9658	0.9762	33.30	0.9603	0.9729	32.61	0.9528	0.9690
	ETRPCA	36.33	0.9768	0.9837	35.64	0.9713	0.9812	33.90	0.9595	0.9739
	PTRPCA	36.73	0.9801	0.9858	35.96	0.9753	0.9833	3		

Dataset	Noise Ratio	10%			20%			30%		
		Methods	PSNR↑	SSIM↑	ERGAS↓	PSNR↑	SSIM↑	ERGAS↓	PSNR↑	SSIM↑
Balloons	TRPCA	42.46	0.9952	36.51	41.38	0.9938	40.83	39.91	0.9914	46.76
	ETRPCA	46.46	0.9970	25.03	45.00	0.9961	28.32	42.00	0.9934	38.08
	PTRPCA	47.25	0.9976	23.38	45.63	0.9969	26.75	44.30	0.9959	30.06
	FGTRPCA	<u>51.75</u>	<u>0.9986</u>	<u>12.06</u>	48.20	0.9967	17.56	45.67	0.9953	23.99
	t-CTV	48.40	0.9981	20.53	47.44	0.9977	22.56	46.29	0.9972	25.36
	RTCTV	51.26	0.9980	15.11	50.58	0.9978	15.89	48.46	0.9975	19.01
	SFGTRPCA	60.91	0.9995	6.06	57.26	0.9991	7.98	53.51	0.9987	11.43
Beads	TRPCA	34.16	0.9788	102.24	32.38	0.9691	121.56	30.45	0.9438	147.31
	ETRPCA	38.39	0.9879	65.87	36.34	0.9795	78.55	32.15	0.9495	118.41
	PTRPCA	38.01	0.9880	66.18	36.39	0.9828	77.30	33.15	0.9461	104.36
	FGTRPCA	<u>39.74</u>	<u>0.9889</u>	<u>48.25</u>	<u>36.45</u>	<u>0.9779</u>	<u>69.76</u>	<u>33.29</u>	<u>0.9560</u>	<u>100.96</u>
	t-CTV	37.25	0.9864	68.58	35.96	0.9824	77.49	34.59	0.9757	88.79
	RTCTV	44.30	0.9933	39.30	41.68	0.9892	43.76	37.08	0.9746	66.80
	SFGTRPCA	46.96	0.9964	27.22	43.00	0.9899	37.16	39.51	0.9834	56.09
Cd	TRPCA	31.85	0.9861	143.64	31.02	0.9838	158.19	29.90	0.9803	180.99
	ETRPCA	35.34	0.9908	96.50	34.42	0.9889	106.52	32.58	0.9839	131.50
	PTRPCA	34.99	0.9913	100.59	34.07	0.9895	111.03	33.15	0.9871	123.51
	FGTRPCA	<u>40.72</u>	<u>0.9951</u>	<u>53.67</u>	<u>38.76</u>	<u>0.9875</u>	<u>65.74</u>	<u>36.34</u>	<u>0.9748</u>	<u>85.17</u>
	t-CTV	37.64	0.9932	74.43	37.12	0.9922	78.64	36.56	0.9909	83.77
	RTCTV	40.71	0.9952	51.73	40.65	0.9948	52.32	38.75	0.9928	64.95
	SFGTRPCA	44.26	0.9981	36.15	43.86	0.9928	36.47	41.35	0.9907	48.61
Chart	TRPCA	43.75	0.9928	47.54	41.93	0.9908	53.74	39.94	0.9874	61.15
	ETRPCA	47.78	0.9949	35.86	45.82	0.9936	39.55	41.77	0.9894	50.52
	PTRPCA	48.84	0.9958	33.58	46.63	0.9947	37.13	44.57	0.9927	41.87
	FGTRPCA	<u>51.62</u>	<u>0.9977</u>	21.16	47.15	<u>0.9961</u>	29.09	43.82	0.9922	37.74
	t-CTV	48.52	0.9958	33.22	46.86	0.9950	35.69	44.89	0.9939	39.24
	RTCTV	51.86	0.9962	27.99	50.67	0.9957	<u>28.36</u>	47.76	0.9948	35.81
	SFGTRPCA	60.30	0.9982	<u>24.24</u>	55.66	0.9973	26.25	52.04	0.9955	33.10
Clay	TRPCA	48.83	0.9973	32.69	47.46	0.9965	36.38	45.75	0.9952	42.60
	ETRPCA	52.60	0.9983	24.19	50.98	0.9979	26.67	47.63	0.9963	34.46
	PTRPCA	54.63	0.9988	21.98	52.58	0.9984	24.44	50.43	0.9978	28.18
	FGTRPCA	<u>59.46</u>	<u>0.9995</u>	<u>10.69</u>	55.41	0.9990	16.92	52.53	0.9981	21.46
	t-CTV	55.01	0.9989	19.51	53.61	0.9986	21.58	52.02	0.9983	23.95
	RTCTV	56.54	0.9988	15.19	55.66	0.9987	15.85	53.75	0.9984	19.98
	SFGTRPCA	66.38	0.9998	7.31	61.95	0.9995	10.67	58.36	0.9992	17.74
Cloth	TRPCA	44.19	0.9847	36.04	40.77	0.9788	43.32	36.75	0.9608	58.27
	ETRPCA	46.98	0.9874	30.64	42.39	0.9814	37.29	36.99	0.9601	56.74
	PTRPCA	48.79	0.9889	28.42	44.50	0.9850	33.50	37.85	0.9623	51.74
	FGTRPCA	<u>49.24</u>	<u>0.9924</u>	<u>21.88</u>	43.74	<u>0.9871</u>	30.43	39.80	0.9766	43.28
	t-CTV	46.56	0.9876	30.28	43.46	0.9844	34.86	40.46	0.9785	41.86
	RTCTV	49.79	0.9891	26.22	44.98	0.9861	29.48	37.79	0.9635	50.59
	SFGTRPCA	55.45	0.9931	21.50	50.27	0.9903	26.45	45.39	0.9860	31.24
Egyptian	TRPCA	44.53	0.9950	61.16	43.38	0.9936	66.67	41.78	0.9912	75.79
	ETRPCA	49.23	0.9970	40.56	47.53	0.9962	46.85	43.93	0.9929	62.70
	PTRPCA	50.01	0.9977	38.33	48.09	0.9969	43.91	46.19	0.9958	51.22
	FGTRPCA	<u>50.39</u>	<u>0.9985</u>	<u>25.06</u>	48.56	0.9974	31.40	46.57	0.9950	38.61
	t-CTV	48.92	0.9974	36.12	47.93	0.9969	41.12	45.98	0.9960	46.79
	RTCTV	53.97	0.9978	<u>22.52</u>	<u>52.83</u>	<u>0.9975</u>	<u>23.81</u>	49.93	0.9969	30.64
	SFGTRPCA	63.29	0.9994	<u>11.67</u>	58.52	0.9990	14.82	53.33	0.9980	19.27
Feathers	TRPCA	40.50	0.9872	68.71	39.08	0.9844	75.24	37.41	0.9794	84.53
	ETRPCA	43.95	0.9909	50.57	42.53	0.9889	55.81	39.29	0.9826	71.57
	PTRPCA	44.38	0.9920	48.75	42.96	0.9902	53.60	41.34	0.9869	61.71
	FGTRPCA	<u>47.34</u>	<u>0.9956</u>	<u>28.41</u>	43.68	0.9908	37.09	41.32	0.9864	51.99
	t-CTV	45.19	0.9925	44.17	44.01	0.9914	47.60	42.50	0.9898	51.84
	RTCTV	48.43	0.9936	34.19	47.48	0.9930	34.44	44.77	0.9912	41.72
	SFGTRPCA	55.31	0.9976	20.73	51.35	0.9958	29.09	47.43	0.9930	40.57
Flowers	TRPCA	45.27	0.9847	65.33	43.12	0.9810	74.58	40.83	0.9746	87.24
	ETRPCA	49.56	0.9893	46.89	47.31	0.9866	52.56	42.84	0.9782	69.75
	PTRPCA	51.17	0.9909	43.21	48.67	0.9887	48.47	45.19	0.9837	55.86
	FGTRPCA	<u>53.07</u>	<u>0.9958</u>	<u>23.40</u>	48.37	0.9917	<u>34.31</u>	44.91	0.9848	48.24
	t-CTV	50.33	0.9918	40.48	48.56	0.9905	44.17	46.52	0.9883	49.16
	RTCTV	53.00	0.9923	33.29	51.32	0.9914	34.64	48.19	0.9895	40.73
	SFGTRPCA	61.20	0.9968	22.58	55.41	0.9939	32.13	50.57	0.9913	35.07
Glass	TRPCA	45.20	0.9965	34.70	43.66	0.9957	38.27	42.13	0.9942	42.67
	ETRPCA	49.18	0.9972	28.07	47.63	0.9967	30.26	44.09	0.9952	37.15
	PTRPCA	50.64	0.9977	26.25	48.89	0.9972	28.42	46.78	0.9965	31.36
	FGTRPCA	<u>53.97</u>	<u>0.9986</u>	<u>16.55</u>	50.21	<u>0.9977</u>	22.64	47.32	0.9961	27.62
	t-CTV	48.40	0.9969	29.18	47.15	0.9965	31.35	45.73	0.9958	34.40
	RTCTV	52.07	0.9974	21.64	51.04	0.9972	<u>22.21</u>	48.33	0.9965	27.02
	SFGTRPCA	59.66	0.9989	13.91	56.22	0.9983	18.22	52.90	0.9976	24.81

Table 7: Quantitative comparisons of MSIs with different noise ratios. Best results are marked bold and second-best results are underlined.